

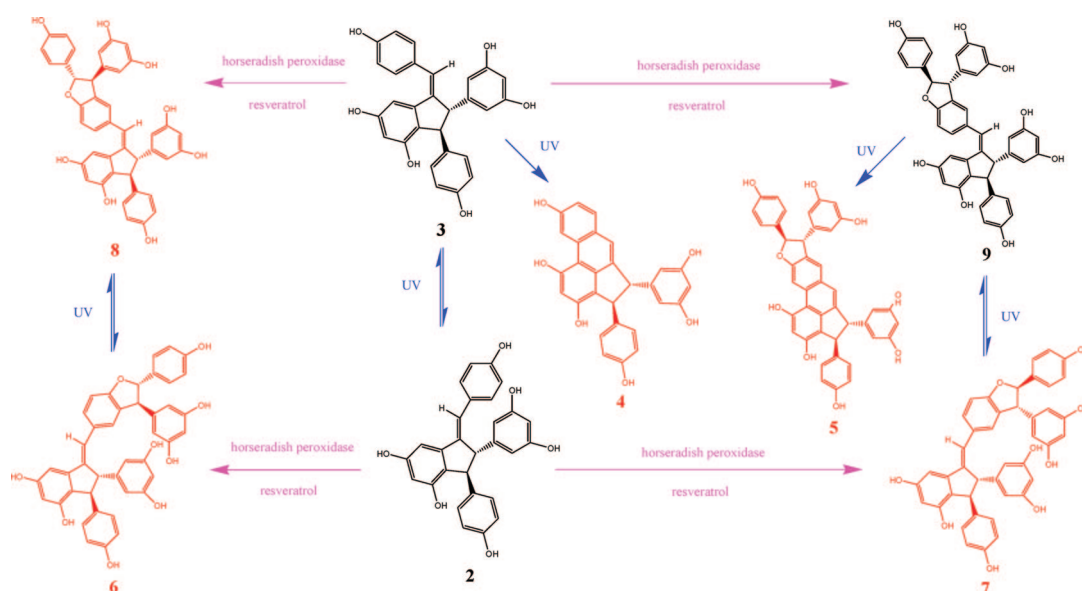
Stilbene Oligomers from *Parthenocissus laetevirens*: Isolation, Biomimetic Synthesis, Absolute Configuration, and Implication of Antioxidative Defense System in the Plant

Shan He, Bin Wu, Yuanjiang Pan,* and Liyan Jiang

Department of Chemistry, Zhejiang University, Hangzhou 310027, China

cheyjpan@zju.edu.cn

Received January 17, 2008



Five new stilbene oligomers, laetevirenol A–E (4–8), were isolated from *Parthenocissus laetevirens*, together with three known stilbene oligomers (2, 3, and 9). The structures of the new compounds were elucidated by spectroscopic analysis, including 1D and 2D NMR experiments. Afterward the absolute configurations were determined. Biomimetic transformations revealed a possible biogenetic route, where stilbene trimers were enzymatically synthesized for the first time. In addition, their antioxidant activities were evaluated by 1,1-diphenyl-2-picrylhydrazyl (DPPH) assay. The results showed that stilbene oligomers with an unusual phenanthrene moiety exhibited much stronger antioxidant activities. Thus, the photocatalyzed cyclization of stilbenes was supposed to be an antioxidant activity promoting transformation, which was hypothesized to play a role in the antioxidative defense system of the plant.

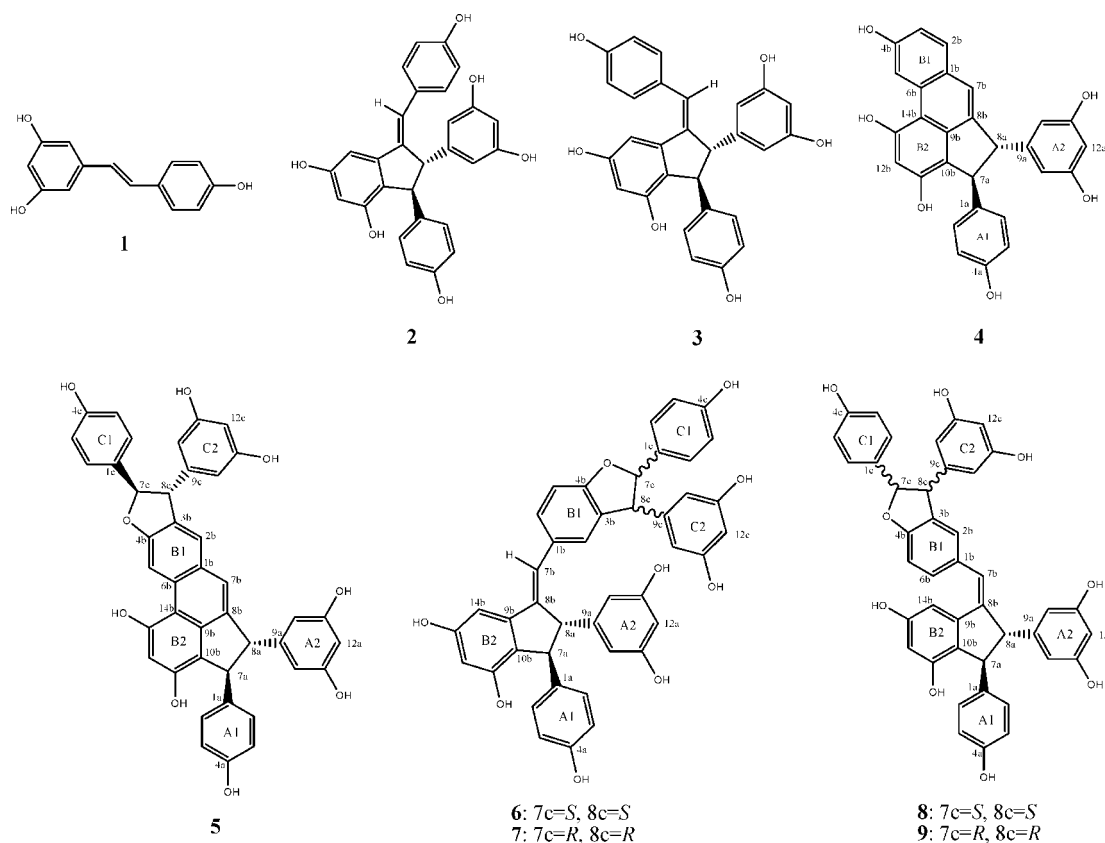
Introduction

Stilbenes are naturally occurring polyphenols found in particular families of plants including Vitaceae, Dipterocarpaceae, Gnetaceae, Cyperaceae, and Leguminosae.¹ They have received considerable attention in the chemical and biological fields, owing to their structural complexity as well as their diverse bioactivities² such as antioxidant,^{3a} cancer chemopre-

ventive,^{3b} anti-inflammatory,^{3c} anti-HIV,^{3d} antifungal,^{3e} anti-mutagenic,^{3f} cytotoxic,^{3g} and hepatoprotective^{3h} activities. By virtue of their potent antioxidant properties and relatively high quantities in red wine,⁴ stilbenes were reported to be responsible, in part, for the so-called “French paradox”—despite a high fat intake, mortality from coronary heart disease was found to be lower in some regions of France due to regular consumption of

(1) Ito, T.; Tanaka, T.; Iinuma, M.; Iliya, I.; Nakaya, K.; Ali, Z.; Takahashi, Y.; Sawa, R.; Shirataki, Y.; Murata, J.; Dardaedi, D. *Tetrahedron* **2003**, *59*, 5347–5363, and references cited therein.

(2) (a) Cichewicz, R. H.; Kouzi, S. A. *Stud. Nat. Prod. Chem.* **2002**, *26*, 507–579, and references cited therein. (b) Lin, M.; Yao, C. S. *Stud. Nat. Prod. Chem.* **2006**, *33*, 601–644, and references cited therein.

CHART 1. Structures of Resveratrol (1), Quadrangularin A (2), Parthenocissin A (3), Laetevirenenol A–E (4–8), and Parthenocissin B (9)

red wine.⁵ Stilbenes are, therefore, potentially useful lead compounds for drug development.

Plants of the genus *Parthenocissus* (Vitaceae) are known to be rich sources of stilbenes, especially resveratrol (1) oligomers.⁶ Stilbenes from *P. tricuspidata* have shown strong antioxidant activities in three different bioassay systems.^{6a} However, phytochemical and pharmacological studies on these plants are still scarce. *P. laetevirens* Rehd. is usually planted as a cover crop in east China and traditionally used as folk medicine for the treatment of rheumatism.⁷ Recently, we have developed a methodology for the isolation and purification of two resveratrol dimers, identified as quadrangularin A (2)⁸ and parthenocissin

A (3),^{6c} from a crude sample of *P. laetevirens* in one-step separation by counter-current chromatography, and their antioxidant activities were found to be stronger than that of vitamin C as determined by the β -carotene bleaching assay.⁹ The following phytochemical investigation on this species led to the isolation of five new resveratrol oligomers, named laetevirenenol A–E (4–8), along with three known compounds (2, 3, and 9) (Chart 1). The structures were established mainly on the basis of 2D NMR spectroscopy, and the absolute configurations were determined. In addition, their biogenetic relationship was revealed by biomimetic transformations. Among the isolates, 4 and 5 showed stronger antioxidant activities due to their phenanthrene moiety, which is unusual in stilbene oligomers. This leads us to the hypothesis that the photocatalyzed cyclization of stilbenes is an antioxidant activity promoting transformation, and that the cyclized compounds might play a role in the antioxidative defense mechanism of the plant. We present these results in the succeeding sections of this paper.

Results and Discussion

The roots and stems of *P. laetevirens* were extracted with methanol at room temperature to yield a crude extract, which was partitioned between ethyl acetate and water. The ethyl acetate solubles were separated by silica gel column chromatography (CC) followed by reversed-phase C-18 CC and semipreparative high-performance liquid chromatography (HPLC) to afford compounds 2–9.

(3) (a) Fang, J.; Lu, M.; Chen, Z.; Zhu, H.; Yang, L.; Wu, L.; Liu, Z. *Chem. Eur. J.* **2002**, *8*, 4191–4198. (b) Jang, M.; Cai, L.; Udeani, G. O.; Slowing, K. V.; Thomas, C. F.; Beecher, C. W. W.; Fong, H. H. S.; Farnsworth, N. R.; Kinghorn, A. D.; Mehta, R. G.; Moon, R. C.; Pezzuto, J. M. *Science* **1997**, *275*, 219–220. (c) Huang, K. S.; Lin, M.; Yu, L. N.; Kong, M. *Tetrahedron* **2000**, *56*, 1321–1329. (d) Dai, J. R.; Hallock, Y. F.; Cardellina, J. H., II; Boyd, M. R. *J. Nat. Prod.* **1998**, *61*, 351–353. (e) Bokel, M.; Diyasena, C.; Gunatilaka, A. A. L.; Kraus, W.; Sotheeswaran, S. *Phytochemistry* **1988**, *27*, 377–380. (f) Uenobe, F.; Nakamura, S.; Miyazawa, M. *Mutat. Res.* **1997**, *373*, 197–200. (g) Ohyama, M.; Tanaka, T.; Ito, T.; Inuma, M.; Bastow, K. F.; Lee, K. H. *Bioorg. Med. Chem. Lett.* **1999**, *9*, 3057–3060. (h) Oshima, Y.; Namao, K.; Kamijou, A.; Matsuoka, S.; Nakano, M.; Terao, K.; Ohizumi, Y. *Experimentia* **1995**, *51*, 63–66.

(4) Vitrac, X.; Bornet, A.; Vanderlinde, R.; Valls, J.; Richard, T.; Delaunay, J.; Mérillon, J.; Teissédre, P. *J. Agric. Food Chem.* **2005**, *53*, 5664–5669.

(5) Renaud, S. C.; Guéguen, R.; Siest, G.; Salamon, R. *Arch. Intern. Med.* **1999**, *159*, 1865–1870.

(6) (a) Kim, H. J.; Saleem, M.; Seo, S. H.; Jin, C.; Lee, Y. S. *Planta Med.* **2005**, *71*, 973–976. (b) Tanaka, T.; Ohyama, M.; Morimoto, K.; Asai, F.; Inuma, M. *Phytochemistry* **1998**, *48*, 1241–1243. (c) Tanaka, T.; Inuma, M.; Murata, H. *Phytochemistry* **1998**, *48*, 1045–1049. (d) Lins, A. P.; Felicio, J. D.; Braggio, M. M.; Roque, L. C. *Phytochemistry* **1991**, *30*, 3144–3146.

(7) Editorial Committee of Flora of Zhejiang. *Flora of Zhejiang*; Zhejiang Sci&Tech Press: Hangzhou, China, 1993; Vol. 4, p 128.

(8) Adesanya, S. A.; Nia, R.; Martin, M.-T.; Boukamcha, N.; Montagnac, A.; Pais, M. *J. Nat. Prod.* **1999**, *62*, 1694–1695.

(9) He, S.; Lu, Y.; Wu, B.; Pan, Y. *J. Chromatogr. A* **2007**, *1151*, 175–179.

TABLE 1. ^1H and ^{13}C NMR Data of Laetevirenos A (**4**) and B (**5**) in Acetone- d_6^a

position	4		5	
	δ_{H} (mult, J in Hz)	δ_{C}	δ_{H} (mult, J in Hz)	δ_{C}
1a		137.5		137.6
2a(6a)	6.89 (2H, d, 8.5)	128.9	6.90 (2H, d, 8.5)	128.9
3a(5a)	6.71 (2H, d, 8.5)	115.9	6.72 (2H, d, 8.5)	115.9
4a		156.6		156.7
7a	4.63 (1H, d, 3.0)	57.8	4.66 (1H, d, 2.9)	57.8
8a	4.28 (1H, d, 3.0)	62.0	4.29 (1H, d, 2.9)	62.1
9a		149.6		149.6
10a(14a)	6.10 (2H, d, 2.2)	106.7	6.11 (2H, d, 2.2)	106.62
11a(13a)		159.5		159.5
12a	6.20 (1H, t, 2.2)	101.6	6.19 (1H, t, 2.2)	101.6
1b		128.1		129.8
2b	7.63 (1H, d, 8.6)	129.9	7.43 (1H, s)	125.2
3b	7.04 (1H, dd, 8.6, 2.5)	115.3		130.5
4b		156.2		159.68 ^b
5b	8.93 (1H, d, 2.5)	112.6	8.98 (1H, s)	106.56
6b		132.2		131.9
7b	7.17 (1H, br s)	122.1	7.21 (1H, s)	122.5
8b		142.6		143.3
9b		142.4		142.3
10b		120.1		120.2
11b		152.5		152.5
12b	6.79 (1H, s)	104.9	6.85 (1H) ^b	105.0
13b		156.9		156.9
14b		111.8		112.2
1c				133.0
2c(6c)			7.28 (2H, d, 8.6)	128.5
3c(5c)			6.86 (2H) ^b	116.1
4c				158.3
7c			5.51 (1H, d, 7.6)	93.8
8c			4.58 (1H, d, 7.6)	58.1
9c				145.5
10c(14c)			6.21 (2H, d, 2.1)	107.4
11c(13c)				159.72 ^b
12c			6.25 (1H, t, 2.1)	102.3

^a ^1H NMR spectra were measured at 500 MHz, and ^{13}C NMR spectra were run at 125 MHz. ^b Overlapping (in the same column).

The molecular formula of laetevirenos A (**4**) was established as $\text{C}_{28}\text{H}_{20}\text{O}_6$, on the basis of NMR and high-resolution electron spray ionization mass spectrometry (HR-ESI-MS) data, which suggested that **4** was a resveratrol dimer. The ^1H NMR and ^1H – ^1H correlation spectroscopy (COSY) spectra showed the presence of two ortho-coupled aromatic signals assignable to a *p*-hydroxyphenyl group in an A_2B_2 type of arrangement, protons of a 3,5-dihydroxyphenyl group in an A_2B type of arrangement, a set of protons coupled in ABX system on a 1,2,4-trisubstituted benzene ring, two singlet aromatic protons, and two mutually coupled aliphatic protons. The 2D NMR spectra, including the analysis of ^1H – ^1H COSY, as well as the heteronuclear multiple quantum correlation (HMQC) and the heteronuclear multiple bond correlation (HMBC) spectra, allowed the assignment of all proton and carbon signals as shown in Table 1, whose structure was deduced mainly from the HMBC spectrum (Figure 1). Correlations of H-2b/C-4b, C-6b; H-3b/C-5b, C-1b; and H-5b/C-1b, C-3b indicated that ring B1 was 1,2,4-trisubstituted. Cross peaks observed between H-7b/C-1b, C-2b, C-6b, C-9b, as well as H-5b/C-14b and H-12b/C-10b, C-14b, revealed the presence of a phenanthrene moiety formed by the cyclization of the resveratrol unit B, as supported by the fact that the proton signal of H-5b (δ 8.93) appeared at a relatively lower field, which was characteristic of the H-5 of a phenanthrene structure.¹⁰ Furthermore, the *p*-hydroxyphenyl group (ring A1) was assigned to be located at C-7a, since HMBC correlations were observed between H-7a/C-2a(6a) and H-8a/C-10a(14a). Finally,

a five-membered ring, consisting of resveratrol unit A and the phenanthrene moiety, was deduced from the HMBC correlations of H-7a/C-10b; H-8a/C-8b; and H-7b/C-8a. As a result, the structure of **4** was determined as shown in Chart 1. To the best of our knowledge, **4** is the first natural occurring resveratrol dimer with a phenanthrene structure. The relative stereostructure was assigned by analysis of the nuclear Overhauser effect spectroscopy (NOESY) spectrum. Nuclear Overhauser effect (NOE) interactions were observed between H-8a/H-2a(6a) and H-7a/H-10a(14a), which demonstrated that the phenyls at C-7a and at C-8a were situated in a trans-orientation to each other.

Laetevirenos B (**5**), obtained as a reddish amorphous powder, was determined to have a molecular formula of $\text{C}_{42}\text{H}_{30}\text{O}_9$ from its HR-ESI-MS, which corresponded to a resveratrol trimer. A comparison between the NMR data of **4** and those of **5** (Table 1, Nos. 1a to 14b) revealed that **4** was probably a partial structure of **5** (resveratrol units A and B). In addition, **5** showed signals (Table 1, Nos. 1c to 12c) corresponding to an additional resveratrol unit C, which was confirmed by HMBC data (Figure 1). HMBC correlations between H-8c/C-3b, C-4b, C-10c(14c) and H-7c/C-2c(6c), C-9c indicated that the resveratrol unit C formed a dihydrofuran ring with the aromatic ring B1, while the *p*-hydroxyphenyl group (ring C1) was substituted at C-7c. The structure of **5** was thus determined as shown in Chart 1. To the best of our knowledge, **5** is the first natural occurring resveratrol trimer identified to possess a phenanthrene structure. Meanwhile, the partial relative stereochemistry was assigned from NOE interactions (Figure 1). NOE interactions observed between H-8a/H-2a(6a) and H-7a/H-10a(14a) showed that the relative configuration of H-7a and H-8a was trans, the same as that of **4**. NOEs observed between H-8c/H-2c(6c) and H-7c/H-10c(14c) indicated that the configuration of the dihydrofuran ring was also trans. However, NOE correlation between H-7a or H-8a with H-7c or H-8c was not observed due to their remote distance.

Laetevirenos C–E (**6**–**8**) manifested the same $[\text{M} - \text{H}]^-$ ion peak at m/z 679 in their ESI-MS. Further HR-ESI-MS evidence demonstrated that they have the same molecular formula as $\text{C}_{42}\text{H}_{32}\text{O}_9$, thereby indicating that they are resveratrol trimers. Their ^1H and ^{13}C NMR spectra were similar to those of parthenocissin B (**9**), previously isolated from *P. quinquefolia*.^{6c} Interestingly, careful analysis of the 2D NMR data of each compound (Figure 2) resulted in the same structure as **9**, revealing that they are stereoisomers of **9** (Table 2). Since each compound had two chiral centers in the dihydrofuran ring (C-7c and C-8c), two chiral centers in the indane moiety (C-7a and C-8a), as well as an asymmetrical double bond (C-7b and C-8b), a NOESY experiment was crucial for structure elucidation (Figure 2). Each compound showed identical NOE correlations between H-8a/H-2a(6a), H-7a/H-10a(14a), H-8c/H-2c(6c), and H-7c/H-10c(14c), thereby indicating that the configurations of both H-7a/H-8a and H-7c/H-8c were determined as trans. However, NOE correlation between H-7a or H-8a and H-7c or H-8c was not observed in each spectrum due to their remote distance. In the NOESY spectra of **6** and **7**, H-7b showed a key NOE correlation with H-14b indicating that the configuration of the double bond was *E*, thus **6** and **7** were diastereoisomers. However, NOE correlations between H-14b/H-6b and H-7b/H-8a were observed in the NOESY spectrum

(10) (a) Leong, Y.-W.; Harrison, L. J.; Powell, A. D. *Phytochemistry* **1999**, *50*, 1237–1241. (b) Leong, Y.-W.; Harrison, L. J. *J. Nat. Prod.* **2004**, *67*, 1601–1603.

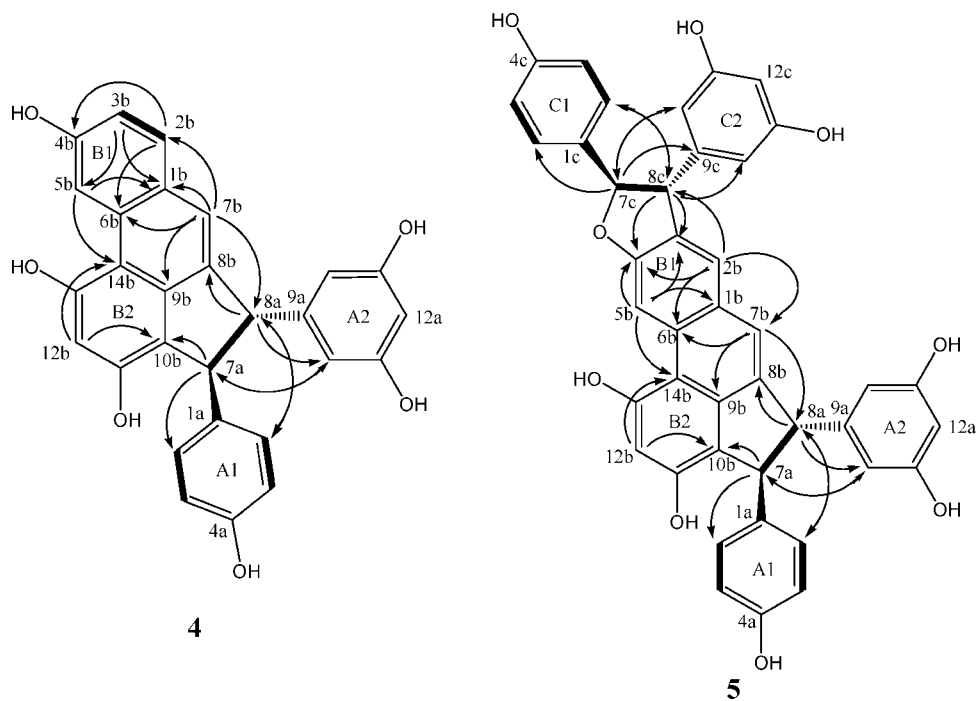


FIGURE 1. Key HMBC (indicated by arrows from ^1H to ^{13}C), ^1H – ^1H COSY (indicated by bold lines), and NOESY correlations (indicated by double-headed arrows between two protons) for **4** and **5**.

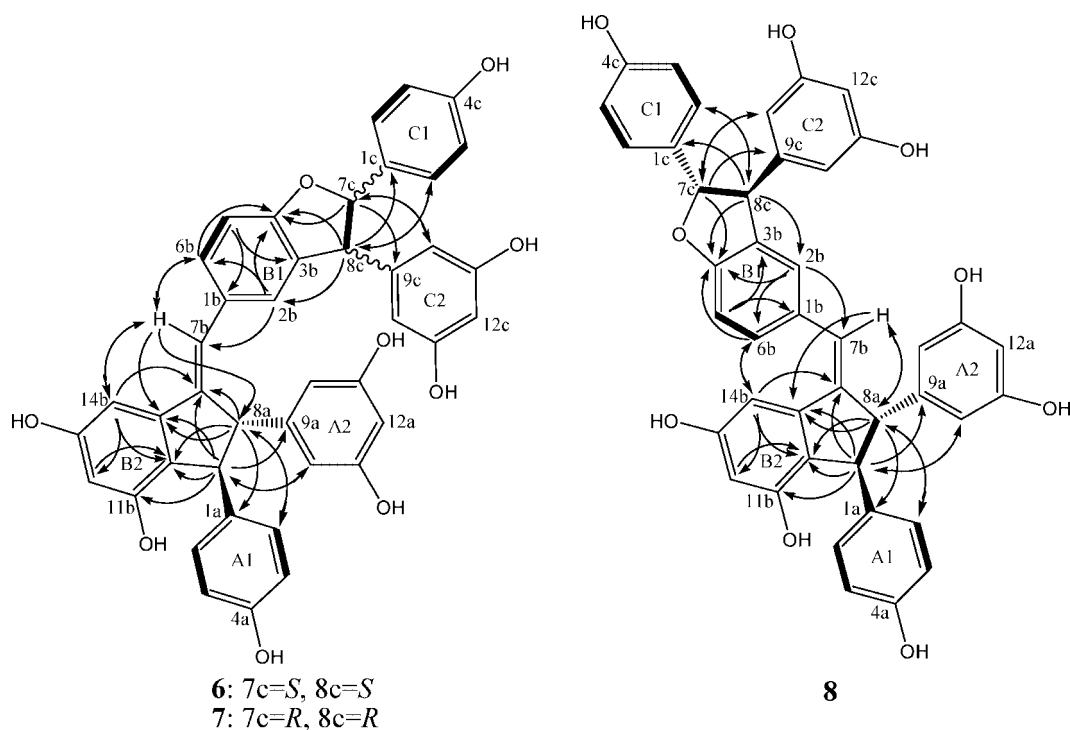


FIGURE 2. Key HMBC (indicated by arrows from ^1H to ^{13}C), ^1H – ^1H COSY (indicated by bold lines), and NOESY correlations (indicated by double-headed arrows between two protons) for **6**, **7**, and **8**.

of **8** demonstrating a *Z* configuration of the double bond, which was the same as that of **9**. Therefore, **8** was a considered diastereoisomer of **9**. As a result, the relative stereochemistries of **6**–**8** were partially determined.

Due to various biological activities of resveratrol and its oligomers, biomimetic cyclodimerizations of resveratrol have been studied extensively by using peroxidase,¹¹ laccase,¹²

grapevine pathogen,¹³ inorganic oxidants,¹⁴ and formic acid.¹⁵ However, study on oxidative coupling of resveratrol with its dimer to generate trimer has not yet been reported. Since all

(11) Takaya, Y.; Terashima, K.; Ito, J.; He, Y.; Tateoka, M.; Yamaguchi, N.; Niwa, M. *Tetrahedron* **2005**, *61*, 10285–10290, and references cited therein.

(12) Nicotra, S.; Cramarossa, M. R.; Mucci, A.; Pagnoni, U. M.; Riva, S.; Forti, L. *Tetrahedron* **2004**, *60*, 595–600.

TABLE 2. ^1H and ^{13}C NMR Data of Laetevirenosol C–E (6–8) in Acetone- d_6^a

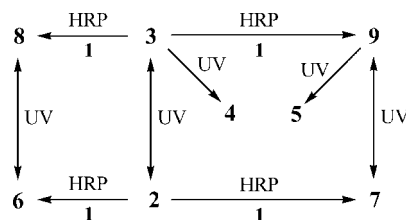
position	6		7		8	
	δ_{H} (mult, J in Hz)	δ_{C}	δ_{H} (mult, J in Hz)	δ_{C}	δ_{H} (mult, J in Hz)	δ_{C}
1a		137.5		137.8		137.3
2a(6a)	6.88 (2H, d, 8.4)	128.7	6.90 (2H, d, 8.5)	128.8	6.98 (2H, d, 8.5)	129.0
3a(5a)	6.66 (2H, d, 8.4)	115.8	6.68 (2H) ^b	115.9	6.71 (2H, d, 8.5)	115.9
4a		156.5		156.6		156.6
7a	4.24 (1H, br s)	57.5	4.27 (1H, br s)	57.5	4.27 (1H, d, 2.6)	54.9
8a	4.07 (1H, br s)	60.8	4.13 (1H, br s)	60.8	3.76 (1H, d, 2.6)	64.5
9a		148.9		149.0		149.6
10a(14a)	6.26 (2H, d, 1.9)	106.4	6.29 (2H, d, 2.2)	106.3	6.19 (2H) ^b	106.7
11a(13a)		159.6 ^b		159.7		159.5
12a	6.21 (1H, t, 1.9)	101.6	6.19 (1H, t, 2.2)	101.7	6.18 (1H) ^b	101.6
1b		131.4		131.5		132.4
2b	7.04 (1H, br s)	127.0	7.01 (1H, br s)	127.7	7.01 (1H, br s)	126.5
3b		131.9		131.7		131.6 ^c
4b		159.5		159.6 ^b		159.9
5b	6.69 (1H, d, 8.4)	109.7	6.68 (1H) ^b	109.7	6.86 (1H) ^b	109.8
6b	7.22 (1H, br d, 8.4)	129.8	7.25 (1H, dd, 1.7, 8.3)	129.4	7.29 (1H, br d) ^b	129.9
7b	7.06 (1H, s)	122.8	7.06 (1H, s)	122.9	6.34 (1H, s)	125.4
8b		143.2		143.4		142.8
9b		147.4		147.4		146.2
10b		124.5		124.6		128.4
11b		155.9		155.9		155.5
12b	6.29 (1H) ^b	103.8	6.30 (1H, d, 2.0)	103.9	6.31 (1H, d, 2.0)	104.6
13b		159.6 ^b		159.6 ^b		158.0
14b	6.79 (1H) ^b	98.4	6.78 (1H, d, 2.0)	98.5	6.61 (1H, d, 2.0)	103.7
1c		132.7		132.7		131.4 ^c
2c(6c)	7.18 (2H, d, 8.5)	128.4	7.17 (2H, d, 8.6)	128.5	7.27 (2H, d, 8.6)	128.8
3c(5c)	6.81 (2H, d, 8.5)	116.1	6.81 (2H, d, 8.6)	116.1	6.87 (2H, d, 8.6)	116.2
4c		158.3		158.4		158.5
7c	5.45 (1H, d, 7.7)	93.3	5.40 (1H, d, 7.8)	93.8	5.42 (1H, d, 8.7)	94.1
8c	4.32 (1H, d, 7.7)	57.7	4.35 (1H, d, 7.8)	57.9	4.51 (1H, d, 8.7)	57.9
9c		145.3		145.2		144.8
10c(14c)	6.16 (2H, d, 1.9)	107.3	6.12 (2H, d, 2.1)	107.3	6.19 (2H) ^b	107.6
11c(13c)		159.66		159.6 ^b		159.7
12c	6.29 (1H) ^b	102.3	6.24 (1H, t, 2.1)	102.4	6.23 (1H, t, 2.1)	102.5

^a ^1H NMR spectra were measured at 500 MHz, and ^{13}C NMR spectra were run at 125 MHz. ^b Overlapping (in the same column). ^c Interchangeable (in the same column).

the isolates in the present study were structurally related, biomimetic transformations were carried out to prove the biogenetic pathway and provide further evidence for the structure elucidation. On the basis of biogenetic considerations, the trimers **6** and **7** were presumed to be formed by the oxidative coupling of the dimer **2** with the monomer **1**. In the present study, treatment of **2** and **1** with horseradish peroxidase (HRP) and hydroperoxide¹⁶ in aqueous acetone gave **6** and **7** each in 14% yield (Scheme 1). To the best of our knowledge, it is the first biomimetic synthesis of resveratrol trimer. Similarly, **8** and **9** were successfully synthesized by oxidative coupling of **3** and **1** with HRP and hydroperoxide under the same condition each in 15% yield (Scheme 1).

From the chemical structure discussed above, we presumed that the phenanthrene moiety in **4** and **5** was formed by cyclization of the resveratrol unit B, which led us to the further hypothesis that **3** and **9** were the biogenetic precursors of **4** and **5**, respectively. Enlightened by previous reports that phenanthrene skeleton could be generated from stilbenes by UV irradiation,¹⁷ we introduced **3** and **9** to photochemical reaction

SCHEME 1. Biomimetic Transformations and Proposed Biogenetic Pathway of Resveratrol Oligomers from *P. laetevirens*



in the present study. UV irradiation of **3** in methanol at room temperature for 2 h afforded **4** (9% yield) and **2** (31% yield) (Scheme 1), while nearly 20% of **3** remained unreacted. As monitored by HPLC, the amount of **3** decreased dramatically during the first 20 min from over 95% to 23%, while the amount of **2**, the trans-isomer of **3**, increased significantly from 0% to 55% in the same duration. They both remained quite stable in the following 100 min (Figure 3). It is apparent that in the first 20 min trans–cis isomerization occurred predominantly, and the reaction has reached equilibrium during this period. In the latter 100 min, the amount of **4** increased in a time-dependent manner. However, continuous UV irradiation for over 8 h would result in decomposition of the compounds (data not shown).

(13) Cichewicz, R. H.; Kouzi, S. A.; Hamann, M. T. *J. Nat. Prod.* **2000**, *63*, 29–33.

(14) Sako, M.; Hosokawa, H.; Ito, T.; Iinuma, M. *J. Org. Chem.* **2004**, *69*, 2598–2600.

(15) Li, X. M.; Huang, K. S.; Lin, M.; Zhou, L. X. *Tetrahedron* **2003**, *59*, 4405–4413.

(16) Ito, J.; Niwa, M. *Tetrahedron* **1996**, *52*, 9991–9998.

(17) (a) Syamala, M. S.; Ramamurthy, V. *J. Org. Chem.* **1986**, *51*, 3712–3715. (b) Roberts, J. C.; Pincock, J. A. *J. Org. Chem.* **2004**, *69*, 4279–4282.

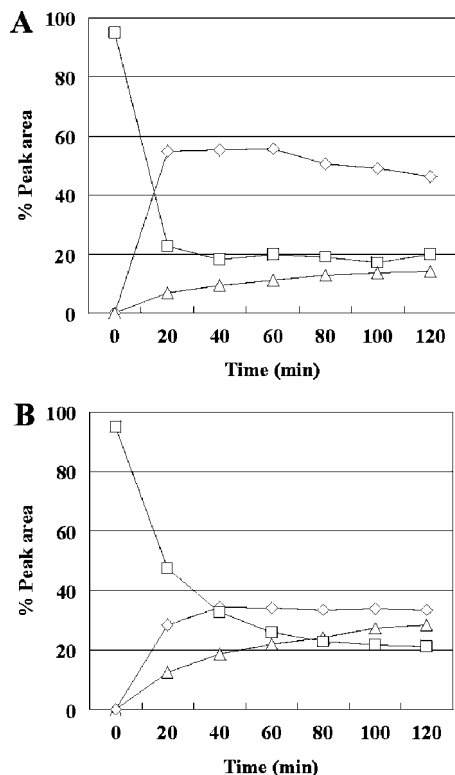


FIGURE 3. UV irradiation of stilbene oligomers were monitored by HPLC with detection at 280 nm. (A, top) Percent peak area versus time plot for the irradiation of the **3** in methanol for 2 h. Products are labeled as follows: **2** (diamonds), **3** (squares), and **4** (triangles). (B, bottom) Percent peak area versus time plot for the irradiation of **9** in methanol for 2 h. Products are labeled as follows: **5** (triangles), **7** (diamonds), and **9** (squares).

Similarly, as a result of UV irradiation of **9**, **5** was generated time dependently (Scheme 1). However, a longer time was needed for **9** and **7** to reach equilibrium (Figure 3). In addition, **6** and **8** could be isomerized to each other under UV irradiation as well (data not shown).

As a result of the above biomimetic transformations, the biogenetic pathway of all the isolates was proposed (Scheme 1). Since the total synthesis of **2** has recently been reported,¹⁸ all the compounds shown in Chart 1 can be totally synthesized.

The relative but not the absolute stereochemistries have been established for the known compounds **2**,⁸ **3**,^{6c} and **9**,^{6c} where they were reported to have trans configurations at 7a/8a chiral centers. Due to the fact that **3** possessed the same skeleton as that of (–)-ampelopsin D (**13**) (Chart 2), whose absolute structure was known,¹⁹ the circular dichroism (CD) spectra of **3** and **13** were compared to determine the absolute configurations. The CD spectrum of **3** showed a strong positive Cotton effect at 246 nm, a positive Cotton effect at 276 nm, and a negative Cotton effect at 332 nm, which exhibited a similar pattern with that of **13**.²⁰ Together with the fact that both **3** and **13** exhibited negative optical rotation, the absolute stereochemistry 7aS,8aR for **3** was therefore established. On the basis of

the biogenetic relationship shown in Scheme 1, compound **2–9** should have the same absolute configurations at the 7a/8a chiral centers, because the biomimetic transformations would not change the absolute configurations.

To determine the absolute configurations of the 7c/8c chiral centers in the resveratrol trimers, **7** was methylated with methyl iodide and potassium carbonate in acetone to afford an octamethyl ether (**7a**), which was then oxidized with ozone to give two degradative products (**11** and **12**) (Scheme 2). The ¹H NMR spectrum of compound **11** (ESI-MS: m/s 391 [M + H]⁺) exhibited the presence of an aldehyde proton as well as a set of ortho-coupled aromatic protons in A₂B₂ systems, a set of meta-coupled protons in A₂B systems, a set of H-atoms coupled in the ABX system on a 1,2,4-trisubstituted benzene ring, three methoxyl groups, and methine protons of a dihydrobenzofuran group. Further analysis of the 2D NMR data, in connection with biogenetic considerations, confirmed the structure of **11**. NOEs observed between H-8c/H-2c(6c) and H-7c/H-10c(14c) indicated that the configuration of the dihydrofuran ring was trans. The CD spectrum of **11** showed a completely opposite pattern to that of gnetin F (**14**) (Chart 2), which has been reported to have a 7'S,8'S configuration from its CD results.²¹ Therefore, the absolute stereochemistry 7cR,8cR for **11** was established. The structure of other degradative product **12** is shown in Scheme 2 and was determined through the 1D and 2D NMR, as well as the HRMS data. On the basis of the biogenetic pathway shown in Scheme 1, the absolute configurations of C-7c and C-8c in **5**, **7**, and **9** should be *R*, since UV-induced isomerization and cyclization would not change the absolute configurations of the chiral centers. On the contrary, **6** and **8** should have a 7cS,8cS configuration, since they were diastereoisomers of **7** and **9** at the 7c/8c chiral centers, respectively. Therefore, we proposed that the absolute structure of compounds **2–9** should be represented as shown in Chart 1.

As an important class of naturally occurring polyphenols, stilbenes are well-known for their antioxidant activities, especially their free radical scavenging properties.²² In recent decades, free radicals have been reported to play a pivotal role in the pathogenesis of numerous diseases, such as stroke, cancer, cardiovascular diseases, and diabetes. Antioxidants like stilbenes, which are able to reduce oxidative stress induced by free radicals, have therefore been considered as one of the most promising therapeutic strategies for the treatment of these diseases.

In the present study, the antioxidant activities of the stilbene oligomers (**2–9**) from *P. laetevirens* together with resveratrol (**1**) were evaluated by DPPH radical assay, widely used for the evaluation of antioxidant activities of natural products.²³ The results presented in Table 3 show that the antioxidant activities of the monomer (**1**) and dimers (**2–4**) were stronger than that of the trimers (**6–9**), except for compound **5**. In addition, among the trimers, the *E*-epimers (**6** and **7**) showed stronger activities than their *Z*-epimers (**8** and **9**). Interestingly, the cyclized compounds, **4** and **5**, which possess a phenanthrene structure, exhibited much stronger activities than **3** and **9**, which were uncyclized. This indicated that the phenanthrene moiety had a great contribution to the antioxidant activity. Therefore, the

(18) Li, W.; Li, H.; Li, Y.; Hou, Z. *Angew. Chem., Int. Ed.* **2006**, *45*, 7609–7611.

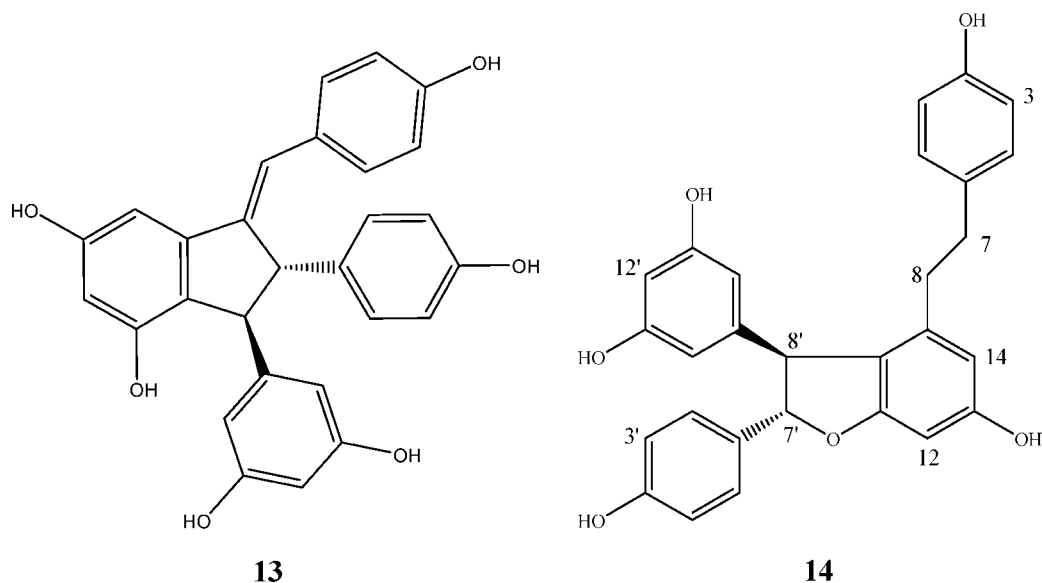
(19) Takaya, Y.; Yan, K. X.; Terashima, K.; Ito, J.; Niwa, M. *Tetrahedron* **2002**, *58*, 7259–7265.

(20) The CD spectrum of (–)-ampelopsin D was reported to show a strong positive Cotton effect at 237 nm, a positive Cotton effect at 272 nm, and a negative Cotton effect at 314 nm in a private communication from Dr. Y. Takaya.¹⁹

(21) Lins, A. P.; Yoshida, M.; Gottlieb, O. R.; Gottlieb, H. E.; Kubitzki, K. *Bull. Soc. Chim. Belg.* **1986**, *95*, 737–748.

(22) (a) Fauconneau, B.; Waffo-Teguo, P.; Huguet, F.; Barrier, L.; Decendit, A.; Merillon, J. M. *Life Sci.* **1997**, *61*, 2103–2110. (b) Wang, Q. L.; Lin, M.; Liu, G. T. *Jpn. J. Pharmacol.* **2001**, *87*, 61–66.

CHART 2. Structures of (–)-Ampelopsin D (13) and Gnetin F (14)



SCHEME 2. Methylation of 7 and Ozonolysis of 7a

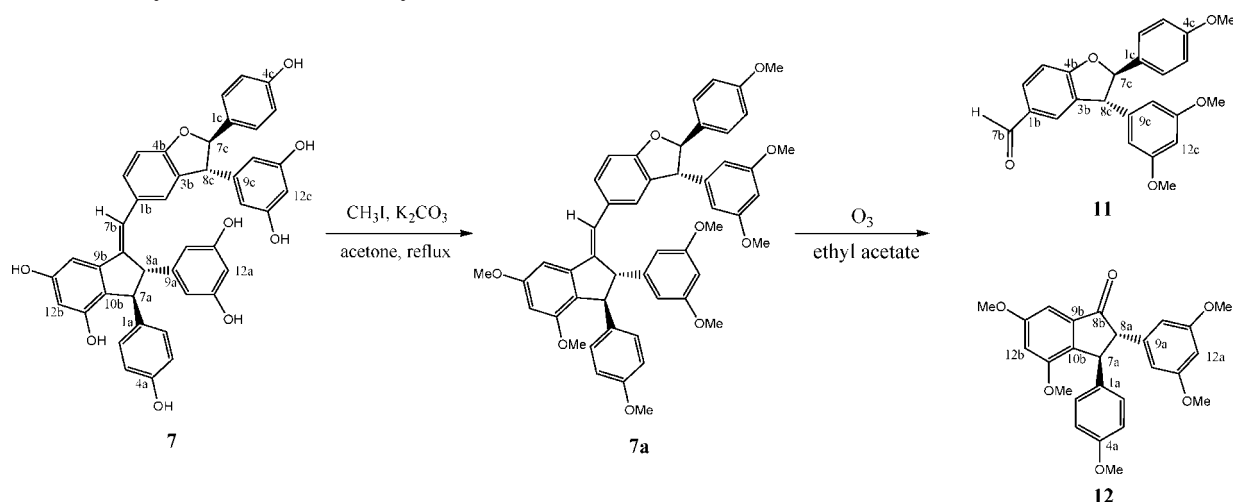


TABLE 3. Antioxidant Activities of the Stilbenes As Determined by DPPH Radical Assay

comps	DPPH radical IC ₅₀ (μM) ^a
1	71.9 ± 1.9
2	66.9 ± 2.0
3	57.9 ± 1.8
4	38.4 ± 1.3
5	37.3 ± 1.4
6	110.8 ± 2.4
7	128.0 ± 2.2
8	158.2 ± 3.1
9	172.7 ± 2.8
vitamin E	28.3 ± 1.2

^a IC₅₀ values were expressed as means ± standard deviation.

photocatalyzed cyclization of stilbenes is probably an antioxidant activity promoting transformation.

When plant tissue is exposed to UV irradiation, the light-dependent generation of reactive oxygen species (ROS), which is termed photooxidative stress, occurs.²⁴ Excessive production of ROS is detrimental to the metabolism in plants, and these reactive molecules can cause damage to plant cellular components including proteins, lipids, and RNA.²⁵ To counteract the

toxicity of ROS, a highly efficient antioxidative defense system, composed of both nonenzymic and enzymic constituents, is present in all plant cells. In addition, some important ROS, such as hydroxyl radical and singlet oxygen, were believed to be detoxified by nonenzymic scavengers and quenchers.²⁶ As it is usually planted as a cover crop, *P. laetevirens* suffers stronger UV irradiation, which is supposed to be linked with its massive production of antioxidants. On the basis of the proposal made above that the photocatalyzed cyclization of stilbenes is an antioxidant activity promoting transformation, we could further hypothesize that *P. laetevirens* is able to directly exploit UV light to generate stronger antioxidants that counteract photooxidative stress induced by UV irradiation. Therefore, this

(23) (a) Lannang, A. M.; Komguem, J.; Ngninzeke, F. N.; Tangmou, J. G.; Lontsi, D.; Ajaz, A.; Choudhary, M. I.; Ranjit, R.; Devkota, K. P.; Sondengam, B. L. *Phytochemistry* **2005**, *66*, 2351–2355. (b) Kolak, U.; Ozturk, M.; Ozgokce, F.; Ulubelen, A. *Phytochemistry* **2006**, *67*, 2170–2175. (c) Luo, X.; Basile, M. J.; Kennelly, E. J. *J. Agric. Food Chem.* **2002**, *50*, 1379–1382.

(24) Asada, K. In *Causes of Photooxidative Stress and Amelioration of Defence Systems in Plants*; Foyer, C. H., Mullineaux, P. M., Eds.; CRC Press: Boca Raton, FL, 1994; pp 77–104.

(25) Casati, P.; Walbot, V. *Plant Cell Environ.* **2005**, *28*, 788–799.

(26) Foyer, C. H.; Lelandais, M.; Kunert, K. J. *Physiol. Plant.* **1994**, *92*, 696–717.

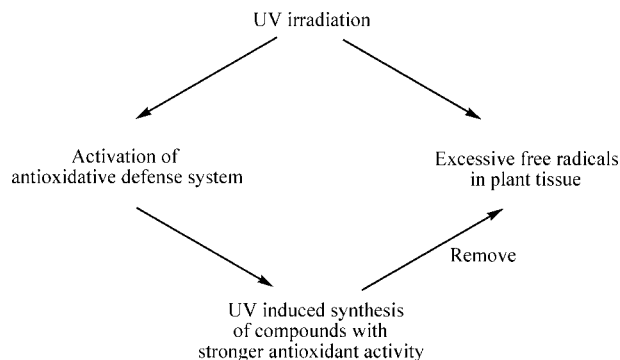


FIGURE 4. Proposed new mechanism of the antioxidative defense system in the plant.

transformation may represent a new mechanism of the antioxidative defense system in the plant, which could enhance the antioxidant capacity in response to photooxidative stress (Figure 4). It is worthy to note that in the current study, all the compounds are from the roots and stems. Additional studies are, therefore, needed for determination of the influence of UV irradiation on the constituents in the leaves (the part of the plant that suffers most from UV) and further investigate this mechanism of antioxidative defense system. Moreover, we also recommend that assays be conducted on the scavenging activities of these compounds on endogenous free radicals in organisms, such as superoxide anion, hydroxyl radical, and singlet oxygen in future investigations.

Experimental Section

Plant Material. The roots and stems of *P. laetevirens* were collected in May 2006 in Hangzhou, Zhejiang Province, China. The material was identified by Dr. Hongxiang Sun (Zhejiang University, Hangzhou, China). A voucher specimen (No. zju 10437) is deposited at the Department of Biology, Zhejiang University, China.

Extraction and Isolation. The dried roots and stems (4.5 kg) of *P. laetevirens* were extracted three times with MeOH (3×15.0 L) at room temperature. The solvent was evaporated in vacuo to afford a concentrated MeOH extract (415 g), which was then diluted with H₂O (1.5 L) to give an aqueous solution (1.5 L). The aqueous solution was extracted with EtOAc three times (3×3.0 L). The combined EtOAc layers were concentrated to dryness in vacuo to provide an EtOAc extract (122 g), which was then subjected to silica gel CC (1200 g, 5 cm diameter) eluted with light petroleum–EtOAc mixtures (100:1 to 1:10) to yield 10 fractions. Fraction 7 (800 mg) was subjected to semipreparative HPLC (column Zorbax Columns Eclipse XDB-C18, 250×9.6 mm i.d.; solvent MeOH–H₂O, 45%:55%; flow rate 3 mL/min; detection 280 nm) to afford five pure isolates **6** ($t_R = 23.0$ min, 5.1 mg), **7** ($t_R = 25.9$ min, 52.6 mg), **5** ($t_R = 48.0$ min, 13.2 mg), **8** ($t_R = 40$ min, 59.6 mg), and **9** ($t_R = 64.4$ min, 264.5 mg). Fraction 8 (6.5 g) was separated by RP-18 CC (MeOH–H₂O, 40%:60%) to give compound **2** (1.2 g), **3** (1.5 g), and **4** (28.1 mg).

Laetevirenol A (4). Yellowish amorphous powder; $[\alpha]_D^{20} +63.7$ (*c* 0.35, Me₂CO); UV (MeOH) λ_{max} (log ϵ) 224.9 (4.5), 261.5 (4.6) nm; IR (KBr) ν_{max} 3404, 2926, 1686, 1654, 1610, 1511, 1449, 1384, 1220, 1158, 1005, 838, 599 cm⁻¹; ¹H and ¹³C NMR data, see Table 1; HR-ESI-MS m/z $[M - H]^-$ 451.1178 (calcd for C₂₈H₁₉O₆, 451.1176).

Laetevirenol B (5). Reddish amorphous powder; $[\alpha]_D^{20} +91.7$ (*c* 0.23, MeOH); UV (MeOH) λ_{max} (log ϵ) 228.5 (4.4), 269.8 (4.6) nm; IR (KBr) ν_{max} 3372, 2926, 1644, 1601, 1513, 1454, 1382, 1305, 1227, 1160, 1104, 1056, 1006, 838, 694, 606 cm⁻¹; ¹H and ¹³C

NMR data, see Table 1; HR-ESI-MS m/z $[M - H]^-$ 677.1814 (calcd for C₄₂H₂₉O₉, 677.1806).

Laetevirenol C (6). Colorless amorphous powder; $[\alpha]_D^{20} +77.0$ (*c* 0.16, MeOH); UV (MeOH) λ_{max} (log ϵ) 222.1 (4.4), 285.2 (3.8), 331.6 (4.1), 346.2 (4.0) nm; IR (KBr) ν_{max} 3369, 1601, 1512, 1487, 1336, 1233, 1150, 1101, 1058, 999, 835, 691, 584 cm⁻¹; ¹H and ¹³C NMR data, see Table 2; HR-ESI-MS m/z $[M - H]^-$ 679.1937 (calcd for C₄₂H₃₁O₉, 679.1963).

Laetevirenol D (7). Colorless amorphous powder; $[\alpha]_D^{20} -34.6$ (*c* 0.25, MeOH); UV (MeOH) λ_{max} (log ϵ) 221.7 (4.4), 286.3 (3.8), 330.4 (4.1), 346.2 (4.0) nm; IR (KBr) ν_{max} 3373, 1601, 1512, 1487, 1340, 1240, 1152, 1106, 1005, 837, 692, 545 cm⁻¹; ¹H and ¹³C NMR data, see Table 2; HR-ESI-MS m/z $[M - H]^-$ 679.1933 (calcd for C₄₂H₃₁O₉, 679.1963).

Laetevirenol E (8). Colorless amorphous powder; $[\alpha]_D^{20} +81.1$ (*c* 0.17, MeOH); UV (MeOH) λ_{max} (log ϵ) 223.1 (4.4), 282.8 (3.7), 311.3 (3.7) nm; IR (KBr) ν_{max} 3373, 1603, 1513, 1484, 1458, 1340, 1239, 1149, 1106, 1004, 836, 692, 547 cm⁻¹; ¹H and ¹³C NMR data, see Table 2; HR-ESI-MS m/z $[M - H]^-$ 679.1937 (calcd for C₄₂H₃₁O₉, 679.1963).

Compounds **2**, **3**, and **9** were determined as (–)-quadrangularin A ($[\alpha]_D^{20} -6$ (*c* 0.25, MeOH)), (–)-parthenocissin A ($[\alpha]_D^{20} -4$ (*c* 0.19, MeOH); CD (MeOH) $\Delta\epsilon$ (nm): +8.39 (246), +1.77 (276), –0.64 (332)) and (–)-parthenocissin B ($[\alpha]_D^{20} -29$ (*c* 0.24, MeOH)) by analysis of the spectroscopic data including optical rotation and comparison with those in the literature.^{6c,8} All the compounds isolated as well as compound **1** were detectable in the extract of fresh material by HPLC/MS (see Figure S49 in the Supporting Information), demonstrating that they were not artifacts.

Treatment of Resveratrol Dimers and Resveratrol (1) with Horseradish Peroxidase (HRP). A mixture of **1** (15 mg), **2** (30 mg), and HRP (0.1 mg) in 50% aqueous acetone (10 mL) was stirred at 25 °C for 5 min. Then 30% H₂O₂ (50 μ L) was added to the reaction solution. After 30 min, the reaction solution was extracted with EtOAc. The organic layer was washed by water and brine, dried over anhydrous magnesium sulfate, concentrated, and then separated by semipreparative HPLC with a C-18 column (Shimadzu), using a mixed solvent of methanol/water 40%:60%, to give **6** (6.3 mg) and **7** (6.4 mg). With a similar procedure to those of **1** and **2**, the treatment of **1** (15 mg) and **3** (30 mg) with HRP and H₂O₂ yielded **8** (6.7 mg) and **9** (6.8 mg).

Photochemical Reaction. All the experiments were carried out in a Pyrex glass-made reactor (30 mL), thermostated at 20 °C. The stirred solution containing **3** (10 mg) in MeOH (10 mL) was irradiated by a Mercury lamp (300 W, $\lambda > 320$ nm, Shanghai Yamin), which had been turned on for at least 30 min. At 20-min intervals of irradiation, small aliquots were withdrawn and analyzed by HPLC [column Agilent Extend C18, 150×4.6 mm i.d., 3.5 μ m particle size; flow rate 0.8 mL/min; solvent 35–40% MeOH in H₂O (0–15 min); detection 280 nm]. After the reaction was complete (120 min), the solvent was removed under reduced pressure, and the residue was taken up in MeOH for separation by semipreparative HPLC with a C-18 column (Shimadzu), using a mixed solvent of methanol/water 40%:60%, to yield **2** (3.1 mg) and **4** (0.9 mg). With a similar procedure to that of **3**, the irradiation of **9** (10 mg) yielded **5** (2.1 mg) and **7** (2.4 mg), except with a mixed solvent of methanol/water 50%:50% for separation. The reaction was monitored by HPLC with similar chromatographic conditions except with a gradient of solvent 45–55% MeOH in H₂O (0–15 min). In addition, **6** and **8** were isomerized from each other under irradiation evidenced by HPLC analysis.

Methylation of 7. A mixture of **7** (40 mg), methyl iodide (0.6 mL), and anhydrous potassium carbonate (0.8 g) in acetone (15 mL) was refluxed for 10 h under nitrogen atmosphere. The mixture was diluted with H₂O and extracted with EtOAc. The extract was washed with H₂O, dried over sodium sulfate, concentrated, and then separated by preparative TLC with light petroleum–EtOAc (2:1, *R_f* 0.49) to give an octamethyl ether (**7a**) (20.4 mg, 44% yield).

7a: Colorless amorphous powder; $[\alpha]_D^{20} +29.6$ (*c* 0.56, CHCl_3); UV (MeOH) λ_{max} (log ϵ) 224.9 (4.4), 285.8 (3.8), 331.6 (4.0), 346.2 (3.9) nm; IR (KBr) ν_{max} 2954, 2926, 2852, 1595, 1511, 1484, 1462, 1428, 1302, 1248, 1203, 1154, 1066, 1034, 831, 693, 538 cm^{-1} ; HR-ESI-MS m/z $[\text{M} + \text{Na}]^+$ 815.3186 (calcd for $\text{C}_{50}\text{H}_{48}\text{O}_9\text{Na}$, 815.3191); ^1H NMR (CDCl_3 , 500 MHz) δ 7.00 (2H, d, $J = 8.6$ Hz, H-2a and H-6a), 6.74 (2H, d, $J = 8.6$ Hz, H-3a and H-5a), 4.24 (1H, br s, H-7a), 4.19 (1H, br s, H-8a), 6.26 (2H, d, $J = 1.9$ Hz, H-10a and H-14a), 6.14 (1H, t, $J = 1.9$ Hz, H-12a), 6.90 (1H, br s, H-2b), 6.76 (1H, overlapping, H-5b), 7.20 (1H, overlapping, H-6b), 7.08 (1H, s, H-7b), 6.27 (1H, d, $J = 1.4$ Hz, H-12b), 6.78 (1H, overlapping, H-14b), 7.20 (2H, overlapping, H-2c and H-6c), 6.85 (2H, d, $J = 8.6$ Hz, H-3c and H-5c), 5.35 (1H, d, $J = 8.8$ Hz, H-7c), 4.34 (1H, d, $J = 8.8$ Hz, H-8c), 6.07 (2H, d, $J = 2.0$ Hz, H-10c and H-14c), 6.31 (1H, overlapping, H-12c), 3.74 (3H, s, MeO-4a), 3.62 (6H, s, MeO-11a and MeO-13a), 3.57 (3H, s, MeO-11b), 3.89 (3H, s, MeO-13b), 3.79 (3H, s, MeO-4c), 3.66 (6H, s, MeO-11c and MeO-13c); ^{13}C NMR (CDCl_3 , 125 MHz) δ 138.3 (s, C-1a), 128.1 (2C, d, C-2a and C-6a), 113.9 (2C, d, C-3a and C-5a), 158.1 (s, C-4a), 56.9 (d, C-7a), 59.6 (d, C-8a), 147.6 (s, C-9a), 104.9 (2C, d, C-10a and C-14a), 161.0 (2C, s, C-11a and C-13a), 97.9 (d, C-12a), 130.4 (s, C-1b), 125.8 (d, C-2b), 130.6 (s, C-3b), 159.1 (s, C-4b), 109.6 (d, C-5b), 130.5 (d, C-6b), 122.9 (d, C-7b), 141.9 (s, C-8b), 145.6 (s, C-9b), 127.1 (s, C-10b), 157.7 (s, C-11b), 99.3 (d, C-12b), 161.6 (s, C-13b), 94.9 (d, C-14b), 132.6 (s, C-1c), 127.7 (2C, d, C-2c and C-6c), 114.2 (2C, d, C-3c and C-5c), 159.8 (s, C-4c), 93.4 (d, C-7c), 58.1 (d, C-8c), 143.5 (s, C-9c), 106.1 (2C, d, C-10c and C-14c), 161.0 (2C, s, C-11c and C-13c), 99.5 (d, C-12c), 55.38 (3C, q, OMe-4a, OMe-11c and OMe-13c), 55.2 (2C, q, OMe-11a, OMe-13a), 55.47 (q, OMe-11b), 55.8 (q, OMe-13b), 55.53 (q, OMe-4c).

Ozonolysis of 7a. A solution of **7a** (20 mg) in ethyl acetate (20 mL) was cooled at -78°C , treated with ozone for 2 min, and then worked up with dimethyl sulfide (0.5 mL) to give the resulting mixture. The mixture was separated by semipreparative HPLC with C-18 column (Shimadzu), using a mixed solvent of methanol/water 65%:35%, to yield **11** (2.4 mg, 24% yield) and **12** (3.3 mg, 30% yield).

11: colorless amorphous powder; $[\alpha]_D^{20} -62.0$ (*c* 0.58, EtOAc); CD (EtOAc) $\Delta\epsilon$ (nm) +1.3 (302), -44.7 (235); UV (MeOH) λ_{max} (log ϵ) 229.6 (4.4), 281.6 (4.1), 296.3 (4.1) nm; IR (KBr) ν_{max} 3431, 2956, 2918, 2849, 1688, 1604, 1515, 1463, 1247, 1204, 1156, 1102, 1066, 1034, 832, 695, 629 cm^{-1} ; HR-ESI-MS m/z $[\text{M} + \text{Na}]^+$ 413.1369 (calcd for $\text{C}_{24}\text{H}_{22}\text{O}_5\text{Na}$, 413.1359); ^1H NMR (acetone- d_6 , 500 MHz) δ 7.56 (1H, d, $J = 1.5$ Hz, H-2b), 7.08 (1H, d, $J = 8.3$ Hz, H-5b), 7.86 (1H, dd, $J = 8.3, 1.5$ Hz, H-6b), 9.86 (1H, s, H-7b), 7.36 (2H, d, $J = 8.7$ Hz, H-2c and H-6c), 6.97 (2H, d, $J = 8.7$ Hz, H-3c and H-5c), 5.77 (1H, d, $J = 8.4$ Hz, H-7c), 4.68 (1H, d, $J = 8.4$ Hz, H-8c), 6.43 (2H, d, $J = 2.2$ Hz, H-10c and H-14c), 6.45 (1H, t, $J = 2.2$ Hz, H-12c), 3.81 (3H, s, OMe-4c), 3.75 (6H, s, OMe-11c and OMe-13c); ^{13}C NMR (acetone- d_6 , 125 MHz) δ 132.2 (s, C-1b), 127.0 (d, C-2b), 133.2 (s, C-3b), 165.5 (s, C-4b), 110.6 (d, C-5b), 133.5 (d, C-6b), 190.9 (d, C-7b), 132.7 (s, C-1c), 128.6 (2C, d, C-2c and C-6c), 114.9 (2C, d, C-3c and C-5c), 160.9 (s, C-4c), 94.4 (d, C-7c), 57.1 (d, C-8c), 144.2 (s, C-9c), 107.1 (2C, d, C-10c and C-14c), 162.3 (2C, s, C-11c and C-13c), 99.7 (d, C-12c), 55.6 (3C, q, OMe-4c, OMe-11c and OMe-13c).

12: colorless amorphous powder; $[\alpha]_D^{20} +9.1$ (*c* 0.77, CHCl_3); UV (MeOH) λ_{max} (log ϵ) 221.4 (4.5), 271.0 (3.8), 332.8 (3.3) nm; IR (KBr) ν_{max} 2955, 2923, 2851, 1712, 1608, 1512, 1463, 1306, 1249, 1203, 1156, 1109, 1061, 1032, 837, 670, 582 cm^{-1} ; HR-ESI-MS m/z $[\text{M} + \text{Na}]^+$ 457.1625 (calcd for $\text{C}_{26}\text{H}_{26}\text{O}_6\text{Na}$, 457.1622); ^1H NMR (CDCl_3 , 500 MHz) δ 6.94 (2H, d, $J = 8.6$ Hz, H-2a and H-6a), 6.79 (2H, d, $J = 8.6$ Hz, H-3a and H-5a), 4.51 (1H, d, $J = 2.7$ Hz, H-7a), 3.60 (1H, d, $J = 2.7$ Hz, H-8a), 6.23 (2H, d, $J = 2.2$ Hz, H-10a and H-14a), 6.35 (1H, t, $J = 2.2$ Hz, H-12a), δ 6.68 (1H, d, $J = 2.1$ Hz, H-12b), 6.89 (1H, d, $J = 2.1$ Hz, H-14b), 3.78 (3H, s, OMe-4a), 3.73 (6H, s, OMe-11a and OMe-13a), 3.66 (3H, s, OMe-11b), 3.87 (3H, s, OMe-13b); ^{13}C NMR (CDCl_3 , 125 MHz) δ 135.5 (s, C-1a), 127.9 (2C, d, C-2a and C-6a), 113.8 (2C, d, C-3a and C-5a), 158.2 (s, C-4a), 50.9 (d, C-7a), 65.4 (d, C-8a), 141.6 (s, C-9a), 106.1 (2C, d, C-10a and C-14a), 161.0 (2C, s, C-11a and C-13a), 98.9 (d, C-12a), 205.5 (s, C-8b), 138.6 (s, C-9b), 138.5 (s, C-10b), 157.8 (s, C-11b), 106.6 (d, C-12b), 161.9 (s, C-13b), 96.5 (d, C-14b), 55.2 (q, OMe-4a), 55.3 (2C, q, OMe-11a and OMe-13a), 55.6 (q, OMe-11b), 55.8 (q, OMe-13b).

Determination of Antioxidant Activity.²³ The reaction mixture containing 20 μL of sample solution (different concentrations in ethanol) and 180 μL of DPPH (1,1-diphenyl-2-picrylhydrazyl, 150 μM) in ethanol was taken in a 96-well microplate and incubated at 37°C for 30 min. The absorbance was measured at 517 nm by a microplate reader. Percent radical scavenging activity was determined by comparison with an ethanol-containing control and calculated by the following equation:

$$I(\%) = 100 \times (A_{\text{blank}} - A_{\text{sample}}) / A_{\text{blank}} \quad (1)$$

where A_{blank} is the absorbance of the control reaction mixture excluding the test compounds, and A_{sample} is the absorbance of the reaction mixture with the tested compounds. IC_{50} values represent the concentration of compounds to scavenge 50% of DPPH radicals and are expressed as means \pm standard deviation of three separate experiments. Vitamin E was used as a positive control.

Acknowledgment. Financial support from the NSFC (20775069) and the NCET-06-520 is gratefully acknowledged. We thank Prof. Yiming Xu (Zhejiang University) for the photochemical reaction, Prof. Xuan Tian (Lanzhou University) for the CD measurement, Dr. Haining Gu (Zhejiang University) for the ozonolysis experiment, and Dr. Yoshiaki Takaya (Meijo University) for providing the CD spectrum of (–)-Ampelopsin D.

Supporting Information Available: General Experimental Methods, Chemicals, 1D and 2D NMR spectra, as well as HRMS data of compounds **4–8**, ^1H and ^{13}C NMR spectra of **7a**, **11**, and **12**, and CD spectra of **3** and **11**, and HPLC/MS data for the extract of fresh material. This material is available free of charge via the Internet at <http://pubs.acs.org>.

JO8001112